Available online at www.sciencedirect.com
SCIENCE DIRECT®
Journal of Power Sources 142 (2005) 306–312
JOURNAL OF POWER SOURCES
www.elsevier.com/locate/jpowsour

Effect of synthesis condition on the structural and electrochemical properties of $Li[Ni_{1/3}Mn_{1/3}Co_{1/3}]O_2$ prepared by carbonate co-precipitation method

T.H. Cho[a], S.M. Park[a], M. Yoshio[a,*], T. Hirai[b], Y. Hideshima[b]

[a] *Department of Applied Chemistry, Saga University, Honjo 1, Saga 840-8502, Japan*
[b] *Industrial Technology Center of SAGA, Nabeshima 114, Saga 849-0932, Japan*

Received 4 August 2004; received in revised form 18 October 2004; accepted 20 October 2004
Available online 19 December 2004

Abstract

In order to get homogeneous layered oxide $Li[Ni_{1/3}Mn_{1/3}Co_{1/3}]O_2$ as a lithium insertion positive electrode material, we applied carbonate co-precipitation. The oxide compounds were synthesized under different annealing temperature. XRD experiment revealed that the layered $Li[Ni_{1/3}Mn_{1/3}Co_{1/3}]O_2$ material can be synthesized at lower temperature of 750 °C, and the oxidation state of Ni, Mn and Co in the cathode confirmed by XPS were 2+, 4+ and 3+, respectively. SEM observation shows that the synthesized materials have spherical particle morphology and the morphology could be controlled by carbonate co-precipitation method. The cathode synthesized at 800 °C showed small irreversible capacity loss of 10.72% and high discharge capacity of 186.7 mAh g^{-1} as well as stable cycling performance in the voltage range 2.8–4.5 V_{Li/Li^+}. In spite of difference in specific surface area, rate capability of the samples synthesized in the temperature range 750–900 °C showed similar rate capability and all these cathodes delivered high discharge capacity of over than 143 mAh g^{-1} at 2.5 C (450 mA g^{-1}).

Keywords: Lithium-ion battery; Carbonate co-precipitation; XPS; Rietveld; $Li[Ni_{1/3}Mn_{1/3}Co_{1/3}]O_2$

1. Introduction

$LiCoO_2$ has been used a major cathode material for lithium ion secondary battery since Sony firstly introduced $LiCoO_2$ as a cathode material. Obviously, it is excellent cathode material with low irreversible capacity loss and good cycling performance. The practical capacity of lithium ion battery has been increased gradually by intensive research for both cathode and anode materials. However, the newly developed multi-functional portable devices need high volumetric energy density over $LiCoO_2$, moreover, cobalt price became more expensive nowadays. These drawbacks accelerate intensive study to find alternative cathode material.

Recently, a layered transition metal oxide with hexagonal structure, $Li[Ni_{1/3}Mn_{1/3}Co_{1/3}]O_2$, was introduced by Ohzuku and Makimura as a candidate of cathode material to be replaced $LiCoO_2$ [1]. This material attracts significant interest because the combination of nickel, manganese and cobalt can provide advantages such as higher reversible capacity with milder thermal stability at charged state [2], lower cost and less toxicity than $LiCoO_2$. Thus, this solid solution could be one of the promising cathode materials. Unfortunately, it is difficult to prepare this complicated material and this material could show low rate capability depending on the synthetic route. Therefore, it is important for $Li[Ni_{1/3}Mn_{1/3}Co_{1/3}]O_2$ to select suitable preparation method.

To synthesize the cathode material, many researchers applied hydroxide co-precipitation method [2–5]. In hydroxide co-precipitation method, Mn ion is precipitated $Mn(OH)_2$ (Mn is 2+) but oxidized gradually, so valence state changed to Mn^{3+} (MnOOH) or Mn^{4+} (MnO_2) in aqueous solution. Therefore, preparing the precursor reproductively is very difficult. However, in carbonate co-precipitation method,

* Corresponding author. Tel.: +81 952 28 8673; fax: +81 952 28 8591.
E-mail address: yoshio@ccs.ce.saga-u.ac.jp (M. Yoshio).

0378-7753/$ – see front matter © 2004 Elsevier B.V. All rights reserved.
doi:10.1016/j.jpowsour.2004.10.016

valence state of Mn ion is always 2+ and stable in aqueous solution thereby very effective for industrial application owing to increase of reproducibility.

In our previous work, we successfully introduced one of the simplest synthetic method, viz., carbonate co-precipitation method, to prepare a $Li[Ni_{1/3}Mn_{1/3}Co_{1/3}]O_2$ cathode material [6]. When we used this method, homogeneous material could be readily obtained with relatively short preparation time and particle size and/or shape also could be controlled. In the study [6], we only reported structural and electrochemical properties of the cathode material prepared at high temperature of 950 °C. Therefore, it is necessary to study that the effect of preparation condition on the structural and electrochemical properties. Here, therefore, we report structural, morphological and electrochemical properties of layered $Li[Ni_{1/3}Mn_{1/3}Co_{1/3}]O_2$ cathode materials synthesized under different condition by carbonate co-precipitation method.

2. Experimental

For preparing transition metal carbonate powder $Mn_{1/3}Ni_{1/3}Co_{1/3}CO_3$, we used $MnSO_4{\cdot}4–5H_2O$, $NiSO_4{\cdot}6H_2O$, $CoSO_4{\cdot}7H_2O$ and Na_2CO_3 as the starting materials. The detail precipitation route was well described in our previous work [7]. The co-precipitated carbonate powder $Mn_{1/3}Ni_{1/3}Co_{1/3}CO_3$, here after referred as a precursor, was pre-heated at 500 °C for 5 h in air. After pre-heating, we applied EDTA titration to decide exact amount of transition metal ions in the pre-heated powder. To synthesize $Li[Mn_{1/3}Ni_{1/3}Co_{1/3}]O_2$ material, a stoichiometric amount of lithium was mixed with the pre-heated powder and calcined at various temperature for 15 h in air.

X-ray diffraction measurements for the precursor and the synthesized $Li[Mn_{1/3}Ni_{1/3}Co_{1/3}]O_2$ materials were carried out using a Cu Kα radiation of Rigaku Rint 1000 diffractormeter. The XRD data for the cathode materials were carefully collected by step of 0.03° with a constant counting time of 10 s per step. In order to investigate the structural change, we applied Rietveld refinements analysis using the FullProf 2000 program [8]. The chemical composition of the synthesized materials was determined by an inductively coupled plasma spectrometer (ICP: SPS 7800, Seiko instruments, Japan). The specific surface areas of the synthesized materials measured using a Micromeritics Gemini 2375 (USA) by the BET method. Scanning electron microscopy (SEM: JSM-5300E, JEOL, Japan) was carried out to observe the morphologies of the synthesized materials. X-ray photoelectron spectra of the transition metals in the synthesized materials were measured using PHI 5800 (ULVAC-PHI Inc., USA) spectrometer with monochromatic Al Kα radiation. Charge referencing was done with carbon C 1s binding energy of 284.5 eV.

The electrochemical characterizations were carried out using the CR-2032-type coin cell. A cathode was prepared by pressing active material film, which is consist of 20 mg active material and 12 mg conducting binder (Teflonized acetylene black), on the stainless steel mesh. The coin type cell was composed of the cathode, the lithium foil as an anode and 1 M $LiPF_6$-EC/DMC (1:2 in volume) as an electrolyte. The electrochemical cycling tests were performed at room temperature. Cyclic voltammetry study was conducted using a three-electrode cell with 1 M $LiPF_6$-EC/DMC (1:2 in volume) as electrolyte and lithium foil was used as both counter electrode and reference. CV experiments were carried out at a scan speed of 0.1 mV s^{-1} between 2.8 and 4.6 V versus Li/Li^+.

3. Results and discussion

Through the co-precipitation process, we obtained pink colored powder as a precursor. In order to characterize the precursor, X-ray diffraction experiment, SEM observation and ICP spectroscopy were employed. The XRD pattern of the precursor and ideal $MnCO_3$ pattern (JCPDS 07-0268) as a reference were given in Fig. 1. As shown in Fig. 1, the diffraction pattern of the precursor is well coincided with ideal manganese carbonate pattern though X-ray diffraction pattern shows broad integrated lines. The broad integrated diffraction lines can be attributed to the mixture of transition

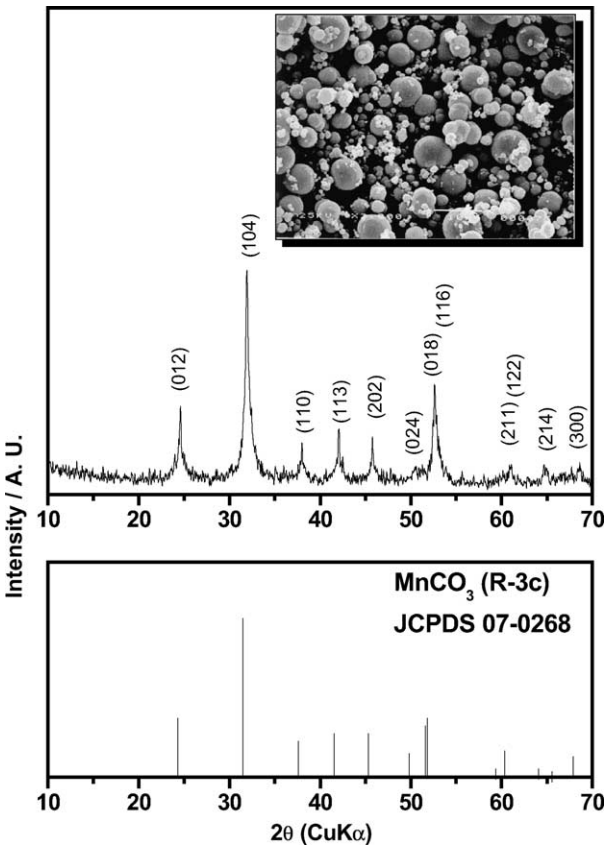

Fig. 1. SEM photograph and X-ray diffraction pattern for co-precipitated powder.

metal carbonates such as $MnCO_3$, $NiCO_3$ and $CoCO_3$. Scanning electron micrograph of the precursor was presented in inset of Fig. 1. The particle morphology of the precursor is spherical with average secondary particle diameter about 5 μm, but primary particle size is less than 1 μm whose particle distribution makes the rate capability to be high. Spherical shape may be due to the constant pH of 7.2, during precipitation. The chemical composition of the precursor from the ICP analysis can be represent as $Mn_{0.34}Ni_{0.33}Co_{0.33}CO_3$ that is almost same as we designed value. Therefore, we could successfully prepare transition metal carbonate precursor by co-precipitation process.

Fig. 2 shows typical XRD patterns of all the synthesized $Li[Mn_{1/3}Ni_{1/3}Co_{1/3}]O_2$ materials at different calcination temperatures, viz., 750, 800, 850, 900 and 950 °C. Hereafter, the materials synthesized at 750, 800, 850, 900 and 950 °C were referred as S75, S80, S85, S90 and S95, respectively. The XRD patterns of all materials can be indexed on the basis of the α-$NaFeO_2$ structure (space group: 166, *R*-3*m*) and no remarkable secondary phase can be observed in the patterns. In the XRD pattern, integrated peak splits of (0 0 6)/(1 0 2) and (0 1 8)/(1 1 0) are known to an indicator of characteristic of layered structure like $LiCoO_2$ and $LiNiO_2$ [9–11]. As can be seen in inset of Fig. 2, regardless of low calcination temperature, the peak splits of (0 0 6)/(1 0 2) and (0 1 8)/(1 1 0) observed in all the XRD patterns which indicate the layered $Li[Ni_{1/3}Mn_{1/3}Co_{1/3}]O_2$ cathode material successfully synthesized at all the calcination temperature in this experiment. Although S75 shows broader diffraction lines than those of the others, the XRD pattern of S75 shows the clear peak splits and there are no impurity phases. These results could be interpreted that homogeneous precursor obtained by carbonate co-precipitation method can be readily synthesized the layered compound even at low temperature of 750 °C.

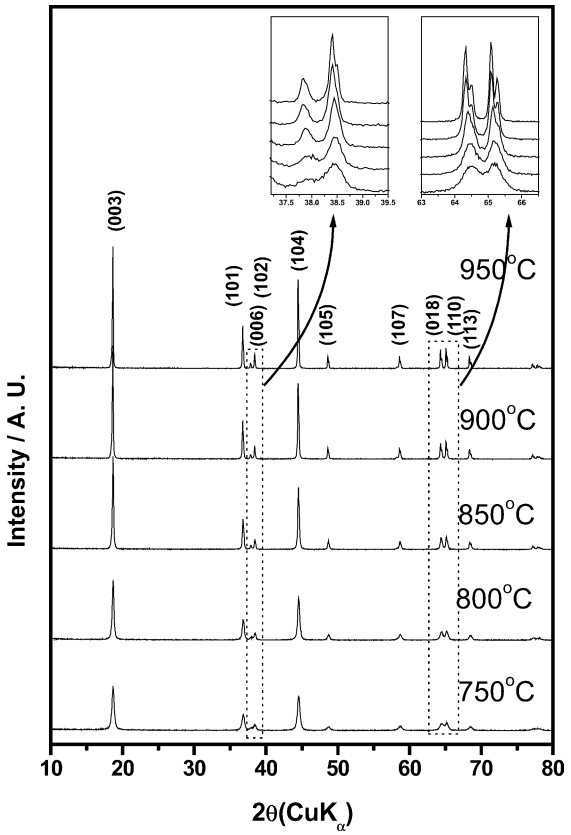

Fig. 2. X-ray diffraction patterns of the synthesized $Li[Mn_{1/3}Ni_{1/3}Co_{1/3}]O_2$ cathode materials.

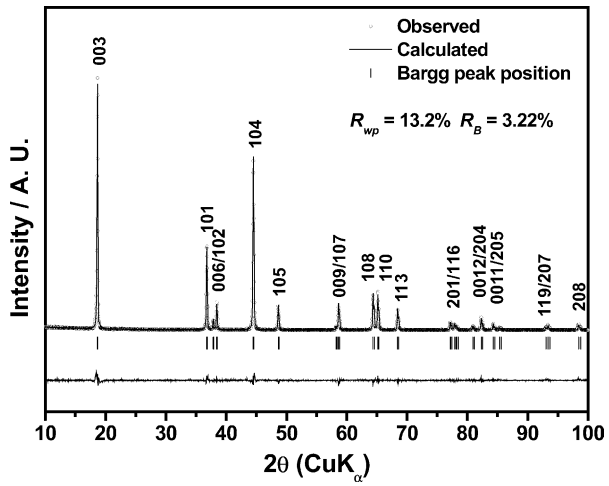

Fig. 3. Rietvelt refinement result of X-ray diffraction pattern for the S90 (synthesized at 900 °C).

Lattice parameters of the synthesized $Li[Mn_{1/3}Ni_{1/3}Co_{1/3}]O_2$ materials were calculated by the Rietveld refinement. Since the scattering power of Mn, Ni and Co are very similar for X-ray, it is hard to distinguish that which ions being occupied the Li site by X-ray pattern refinement. Nevertheless, in this refinement we allowed that only Ni ions could occupy the Li site because several studies reported that only Ni ions could occupy the Li site by neutron and X-ray diffraction profile refinements [12–14]. The profile fit result for S90 was presented in Fig. 3 and obtained parameters are summa-

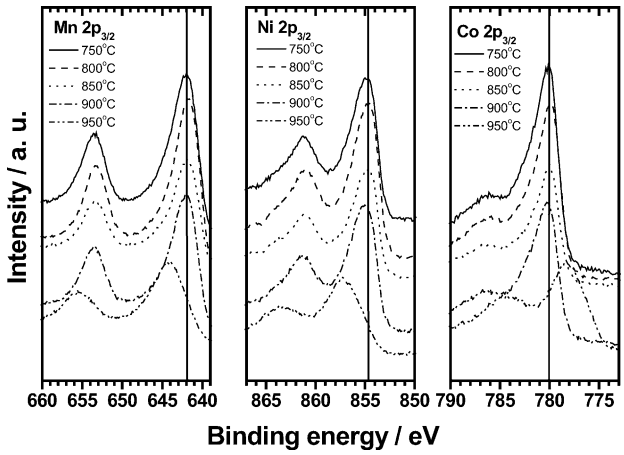

Fig. 4. XPS spectra of Mn $2p_{3/2}$, Ni $2p_{3/2}$ and Co $2p_{3/2}$ for the synthesized $Li[Mn_{1/3}Ni_{1/3}Co_{1/3}]O_2$ cathode materials.

Table 1
Chemical analysis, calculated structure parameters and specific surface area for the synthesized compounds

Calcination temperature (°C)	Composition	Lattice parameter		c/a	Volume	Z_{oxy}	Ni in Li_{3b} site	Reliable factor		Specific surface area ($m^2\ g^{-1}$)
		a (Å)	c (Å)					R_{WP}	R_B	
750	$Li_{1.01}Mn_{0.34}Ni_{0.32}Co_{0.34}O_2$	2.861	14.23	4.97	100.89	0.2594(2)	0.029(3)	13.1	1.96	11.3
800	$Li_{1.01}Mn_{0.34}Ni_{0.32}Co_{0.34}O_2$	2.860	14.23	4.97	100.87	0.2592(1)	0.023(1)	12.5	2.04	9.0
850	$Li_{1.01}Mn_{0.34}Ni_{0.32}Co_{0.34}O_2$	2.861	14.24	4.98	100.97	0.2594(2)	0.015(1)	13.6	3.05	3.0
900	$Li_{1.00}Mn_{0.34}Ni_{0.32}Co_{0.34}O_2$	2.861	14.24	4.98	101.06	0.2593(1)	0.014(1)	13.2	3.22	1.4
950	$Li_{0.98}Mn_{0.34}Ni_{0.32}Co_{0.34}O_2$	2.862	14.25	4.98	101.16	0.2593(2)	0.020(2)	13.1	3.33	0.7

rized in Table 1 . The specific surface area and the chemical analysis result are also summarized in Table 1. As shown in Table 1, with increasing calcination temperature, calculated lattice parameter were somewhat increased. While c/a values that indicate hexagonal structure disorder [12] were virtually unchanged. These results indicate that the specific surface area and lithium content decrease but hexagonal ordering do not change with calcination temperature. Therefore, we believe that the lower calcination temperature could give more advantage in terms of surface area and lithium content.

In order to confirm the oxidation state of the transition metal species in the synthesized $Li[Mn_{1/3}Ni_{1/3}Co_{1/3}]O_2$ materials, XPS study was carried out. Fig. 4 shows XPS results of Mn $2p_{3/2}$, Ni $2p_{3/2}$ and Co $2p_{3/2}$ binding energy. The binding energies of Mn, Ni and Co in the XPS spectra for the S75 were 641.9, 854.5 and 779.9 eV, respectively. From the related studies [5,15], we could confirm that these binding energies of 641.9, 854.5 and 779.9 eV are well coincided with binding energy of Mn^{4+}, Ni^{2+} and Co^{3+}, respectively. Thus, we could say the valence states of Mn, Ni and Co in the S75 are 4+, 2+ and 3+, respectively. Binding energies of all transition metal species in the samples were almost unchanged with increasing calcination temperature up to 900 °C. While, as can be seen in Fig. 4, binding energy of Mn and Ni were

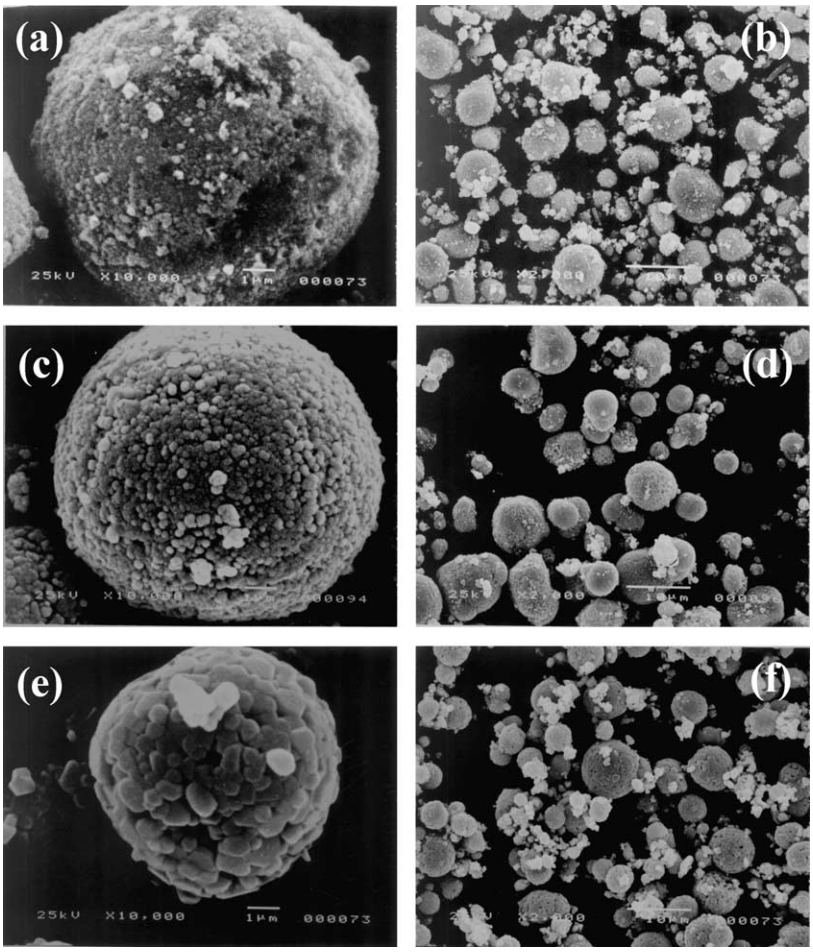

Fig. 5. SEM Photographs for synthesized $Li[Mn_{1/3}Ni_{1/3}Co_{1/3}]O_2$ compounds at 750 °C (a and b), 850 °C (c and d) and 950 °C (e and f).

suddenly increased up to 644 and 857.4 eV when the sample prepared at 950 °C and whereas binding energy of Co was decreased to 778.4 eV in the S95. We could not index the binding energy of Mn and Co because those binding energies are not coinciding with any transition metal species of Mn and Co. Only Ni could be indexed to the Ni^{3+} (Ni_2O_3: 857.3 eV). This result indicates that higher calcination temperature, i.e., 950 °C lead unexpected change of valence state for all the transition metal species. The specific reasons for the change of valence state of transition metals at 950 °C without transforming structure and emerging new phases is not clear yet in this study but we assume that these unexpected changes could be attributed by lithium and oxygen vaporization at high temperature.

In order to observe morphology change of the synthesized $Li[Mn_{1/3}Ni_{1/3}Co_{1/3}]O_2$ materials with calcination temperature, we applied SEM observation at different magnification. Scanning electron micrographs of materials with different calcination temperatures were given in Fig. 5. Fig. 5a, c and e shows the micro morphologies of S75, S85 and S95, respectively. Generally, Small particle (high surface area) can receive high current but tapping density is small. However, as can be seen in Fig. 5a, c and e, the primary particle size is less than 1 μm in diameter and these small particles aggregated each other to form spherical secondary particle. Thus, this kind of morphology could be thought to enhance high rate capability with respect to high surface area without decreasing of tapping density. With increasing calcinations temperature, the primary particles increased up to 1 μm in diameter (Fig. 5e), which leads decrease of surface area. Fig. 5b, d and f shows macro-morphology of the materials. Generally, increasing calcination temperature leads to crystal growth, however macro-morphologies of the materials are almost same and very similar to precursor powder (inset of Fig. 1). Since particle shape and size of cathode material could affect energy density for practical use, controlling particle morphology is very important. As shown in Fig. 5b, d and f, the secondary particle shape or size could be directly controlled by controlling precursor powder. Therefore, we believe that carbonate co-precipitation process is very useful method to prepare cathode material.

Electrochemical charge-discharge experiments of the synthesized $Li[Mn_{1/3}Ni_{1/3}Co_{1/3}]O_2$ materials have been performed at room temperature in the voltage range 2.8 to 4.5 V_{Li/Li^+} with applying current density of 20 mA g^{-1}. Fig. 6a shows first two charge/discharge curves and Fig. 6b shows cycling performance for all the samples up to 30 cycles. As shown in Fig. 6a, the voltage profiles of all the samples are similar to previously reported studies [2,5]. The S75 calcined at 750 °C showed the charge capacity of 205.4 mAh g^{-1} and the discharge capacity of 179.4 mAh g^{-1} at the initial cycle as well as stable cycle performance in the subsequent cycles. Although the S75 has lower crystallinity than the other samples, this cathode could deliver high discharge capacity. On increasing calcination temperature, obtained discharge capacities were gradually decreased except S80. The initial

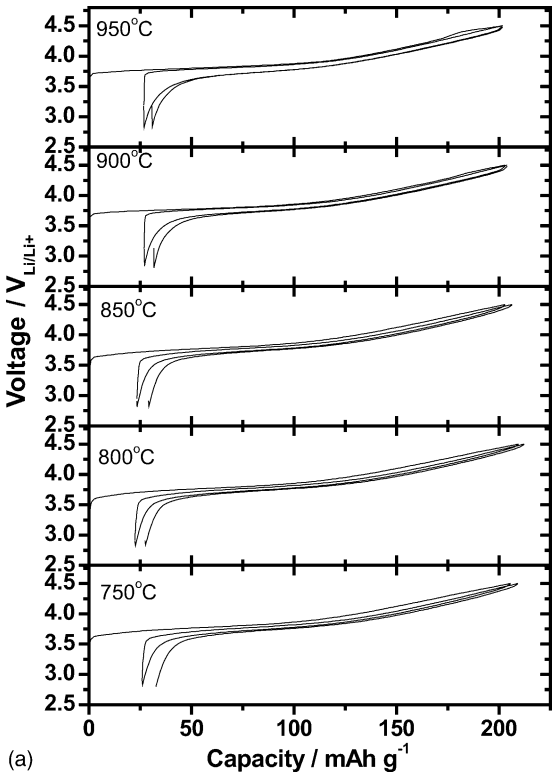

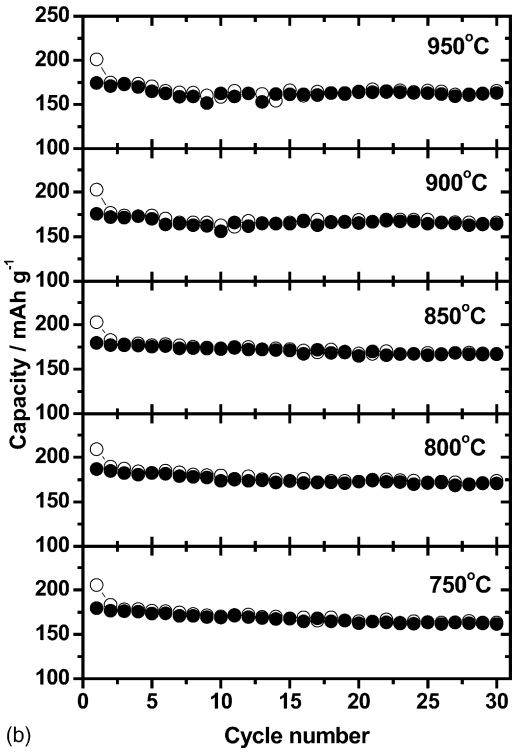

Fig. 6. (a) Charge and discharge curves for initial two cycles and (b) charge–discharge capacities as a function of cycle number of synthesized cathode materials in the voltage range 2.8–4.5 V_{Li/Li^+}.

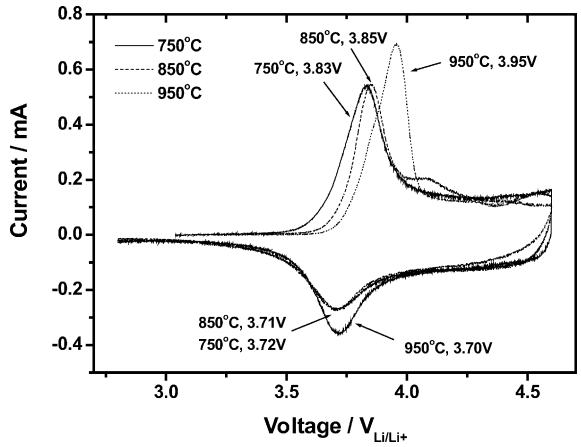

Fig. 7. Cyclic voltammogram of $Li[Mn_{1/3}Ni_{1/3}Co_{1/3}]O_2$ cathode prepared at 750, 850 and 950 °C in the voltage range 2.8–4.6 V_{Li/Li^+}.

discharge capacity of the samples S85, S90 and S95 were 179.3, 175.7 and 174.3 mAh g^{-1}, respectively. The highest initial discharge capacity of 186.7 mAh g^{-1} was obtained by the S80. Moreover, the irreversible capacity loss, which leads shrinkage of energy density in practical use, also slightly increased with increasing calcinations temperature. The irreversible capacity loss of S75, S85, S90 and S95 were 12.7, 11.53, 13.27 and 13.75%, respectively. The smallest irreversible capacity loss of 10.72% was also obtained by S80 calcined at 800 °C. We thought the reasons for the decrease of initial discharge capacity and increasing irreversible capacity loss is due probably to the decrease of lithium content with increasing calcination temperature. However, average capacity retention ratio was slightly increased with increasing calcinations temperature. The average capacity retention ratios of S75, S80, S85, S90, S95 were 99.64, 99.69, 99.75, 99.76 and 99.77% per each cycle, respectively. We thought that S80 calcined at 800 °C shows best electrochemical properties because of moderate crystallity, large surface area and low lithium volatilization.

Fig. 7 shows typical cyclic voltammogram of the S75, S85 and S95. As shown in Fig. 3, major oxidation peak of S75 is 3.83 V_{Li/Li^+} and it shifted to the higher voltage with increasing calcination temperature. It means that the polarization of samples increased with increasing calcinations temperature. Thus, we thought that the increase in the polarization of the samples probably due to increased in cell resistant with respect to specific surface area because the samples calcined at high temperature have smaller specific surface area.

It is well known that rate capability can be affected strongly by surface area of cathode material. In order to elucidate the dependence of rate capability on the surface area (primary particle size) and secondary particle size, we applied 20 mA g^{-1} for charging and 20, 90, 180, 360 and 450 mA g^{-1} for discharge currents across the $Li[Ni_{1/3}Mn_{1/3}Co_{1/3}]O_2$ electrode in the voltage range from 2.8 to 4.5 V_{Li/Li^+}. These current densities can be denoted that 0.11 C (20 mA g^{-1}), 0.5 C (90 mA g^{-1}), 1 C (180 mA g^{-1}),

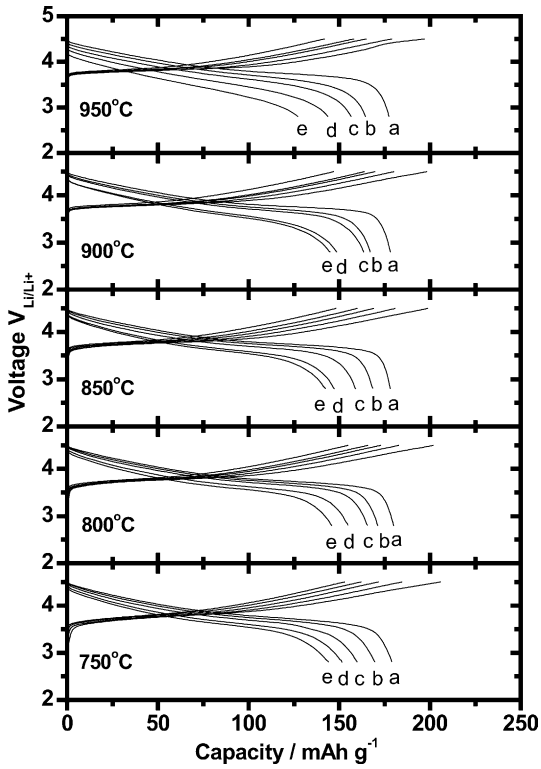

Fig. 8. Rate capability tests for the samples in the voltage range 2.8–4.5 V_{Li/Li^+} (a: 20 mA g^{-1}, b: 90 mA g^{-1}, c: 180 mA g^{-1}, d: 360 mA g^{-1}, e: 450 mA g^{-1}).

2 C (360 mA g^{-1}), 2.5 C (450 mA g^{-1}) and the *C*-rate was calculated using 180 mAh g^{-1} as a theoretical capacity. Fig. 8 shows the results of rate capability experiments. The delivered discharge capacities of S75, S80, S85, S90 and S95 at 2.5 C (450 mA g^{-1}) were 144, 145.7, 142.25, 144.79 and 127.12 mAh g^{-1}, respectively. Surprisingly, S75, S80, S85 to S90 show similar capacity retention ratio at each C-rate in spite of large difference of specific surface area as summarized in Table 1, i.e., S75 has more than eight times larger specific surface area than S90. Our results suggest that the rate capability depends on not the surface area (primary particle size) but the secondary particle size in this study. From the above electrochemical charge/discharge and rate capability tests, we consider that 800 °C is the proper calcination temperature to obtain good cycle stability and rate capability and 950 °C is too high calcination temperature to obtain good rate capability.

4. Conclusion

The layered $Li[Ni_{1/3}Mn_{1/3}Co_{1/3}]O_2$ cathode material with spherical particle shape was successfully synthesized through carbonate co-precipitation method under different calcinations temperature. We could synthesize the homogeneous material even at low temperature of 750 °C and we could control morphology of particles using the co-precipitation

process. All the materials show clear XRD peak splits of (0 0 6)/(1 0 2) and (0 1 8)/(1 1 0) and high *c*/*a* value about 4.97 that means the materials have hexagonal structure. However, from XPS study, the transition metals in the materials are Ni^{2+}, Mn^{4+} and Co^{3+} except sample calcined at 950 °C. From electrochemical experiments, we conclude that 800 °C is an optimal calcination temperature in this experiment and the rate capability of these materials depended on not the surface area (primary particle size) but the secondary particle size.

References

[1] T. Ohzuku, Y. Makimura, Chem. Lett. (2001) 642–643.
[2] N. Yabuuchi, T. Ohzuku, J. Power Sources 119–121 (2003) 171–174.
[3] Z. Lu, D.D. MacNeil, J.R. Dahn, Electrochem. Solid State Lett. 4 (2001) A200–A203.
[4] D.D. MacNeil, Z. Lu, J.R. Dahn, Electrochem. Soc. 149 (2002) A1332–A1336.
[5] K.M. Shaju, G.V. Subba Rao, B.V.R. Chowdari, Electrochim. Acta 48 (2002) 145–151.
[6] T.H. Cho, S.M. Park, M. Yoshio, Chem. Lett. (2004) 700–701.
[7] Y.S. Lee, Y.K. Sun, S. Ota, T. Miyashita, M. Yoshio, Electrochem. Commun. 4 (2002) 989–994.
[8] T. Roisnel, J. Rodriguez-Carjaval, Fullprof Manual, Institut Laue-Langevin, Grnoble, 2000.
[9] J.R. Dahn, U. von sacken, A.V. Chadwick, Solid State Ionics 44 (1990) 87–97.
[10] T. Ohzuku, A. Ueda, M. Nagayama, J. Electrochem. Soc. 140 (1993) 1862–1870.
[11] Y. Gao, M.V. Yakovleva, W.B. Ebner, Electrochem. Solid State Lett. 1 (1998) 117–119.
[12] J.M. Kim, H.T. Chung, Electrochim. Acta 49 (2004) 937–944.
[13] J.M. Kim, H.T. Chung, Electrochim. Acta 49 (2004) 3573–3580.
[14] J. Cho, G. Kim, H.S. Lim, J. Electrochem. Soc. 146 (1999) 3571–3576.
[15] S. Gopukumar, K.Y. Chung, K.B. Kim, Electrochim. Acta 49 (2004) 803–810.